Separation Science and Technology
Publication details, including instructions for authors and subscription information:
http://www.informaworld.com/smpp/title~content=t713708471

Glycine Permeation through Na, Ag, and Cs Forms of Perfluorosulfonated Ion-Exchange Membranes

Meifang Jin[ab]; Subhas K. Sikdar[a]; Scott D. Bischke[a]
[a] CENTER FOR CHEMICAL ENGINEERING NATIONAL BUREAU OF STANDARDS, BOULDER, COLORADO [b] Dalian Institute, People's Republic of China

To cite this Article Jin, Meifang , Sikdar, Subhas K. and Bischke, Scott D.(1988) 'Glycine Permeation through Na, Ag, and Cs Forms of Perfluorosulfonated Ion-Exchange Membranes', Separation Science and Technology, 23: 14, 2293 — 2308
To link to this Article: DOI: 10.1080/01496398808058454
URL: http://dx.doi.org/10.1080/01496398808058454

SEPARATION SCIENCE AND TECHNOLOGY, 23(14 & 15), pp. 2293-2308, 1988

Glycine Permeation through Na^+, Ag^+, and Cs^+ Forms of Perfluorosulfonated Ion-Exchange Membranes

MEIFANG JIN,* SUBHAS K. SIKDAR,† and SCOTT D. BISCHKE

CENTER FOR CHEMICAL ENGINEERING
NATIONAL BUREAU OF STANDARDS
BOULDER, COLORADO 80303-3328

Abstract

We have studied the effect of counterions in perfluorosulfonated ion-exchange membranes on glycine permeation and found that counterions controlled permeation behavior. The Na^+ form of the membrane exhibited saturation kinetics of the Michaelis-Menten type; that is, the flux rapidly increased with concentration and reached a limiting flux at a concentration of about 2 mol/L. The Cs^+ form exhibited markedly lower fluxes which were nearly Fickian. For the Ag^+ form, however, the fluxes increased rapidly and nonlinearly at low concentrations, but attained Fickian linearity at high concentrations. Ionizability of the sulfonate groups and hydration numbers of the counterions appeared to cause departure from Fickian behavior.

INTRODUCTION

Previous permeation studies (*1–5*) of carboxylic and amino acids using perfluorosulfonated ion-exchange membranes have established some potentially useful properties of these membranes. First, the acids permeate through these membranes at different rates—thus providing a basis for selective separation. Second, these acids exhibit saturation kinetics of the Michaelis-Menten type. This fact indicates interactions of the permeating species with the ion-exchange sites of the membrane.

*Present address: Dalian Institute, People's Republic of China.
†To whom correspondence should be addressed.

Third, solution pH can be used to stimulate one species to permeate preferentially.

Most of our previous work dealt with the acid form of the ion-exchange membrane. For example, in acetic acid transport through the acid form of the membrane, we found that acetic acid permeated more rapidly at lower pH's, for example, below its pK, than at pH's above its pK (*2*). Flux therefore increased as acid ionization decreased.

Amino acids permeated more rapidly below their isoelectric pH's. We found this to be true regardless of the type of amino acid (*3*, *4*). In contrast to acetic acid permeation, which increased with the increase of the undissociated form of the acid in solution at low pH's, the amino acid fluxes increased with an increase of the cationic species in solution.

The perfluorosulfonated ion-exchange membranes show promise for separating amino acids from aqueous solutions. Designing suitable permeators will require an understanding of the transport mechanisms together with the ability to predict fluxes. Because of a lack of adequate database, a mechanistic understanding of the permeation behavior of amino acids is yet unavailable.

Varieties of data are needed to determine the transport mechanisms. One important data requirement, to which this study was directed, is the transport behavior of amino acids through membranes that have been altered by replacing the proton of the sulfonic acid by metal ions. This work provides glycine permeation data on membranes with the counterions Na^+, Cs^+, and Ag^+.

In addition to presenting flux data, this study provides insights to transport mechanisms. Specifically we were interested in studying the flux vs concentration data to discriminate the role of the counterions.

Membrane Properties

Perfluorosulfonated ion-exchange membranes possess a polytetrafluoroethylene backbone which is attached, through an ether linkage, to a perfluorinated side chain containing sulfonic acid groups. The sulfonic acid makes the copolymer hydrophilic. The acid form of the membrane is swelled by water to about 30 molecules of water per exchange site at 25°C (*6–8*). The use of the membrane for separations exploits membrane swelling, which opens up the structure of the polymer for permeation.

Various theories for the structure of the perfluorosulfonated ion-exchange membrane exist (*9–11*). One common feature to all these theories is the experimental finding that the membrane structure consists

of hydrophilic clusters, containing the sulfonic acid groups, dispersed in a hydrophobic matrix of perfluorinated polyethylene. The hydrophilic clusters are connected by narrow channels. Ionic solutes are believed to permeate through these channels.

The hydrophilic ion clusters absorb water. This results in membrane swelling, the extent of which depends on the counterion. Water swelling increases with increasing hydration energy of the counterion. Hydration energy can be represented by the hydration number (*12*). Hydration number is the number of water molecules associated with a counterion. A Li^+ membrane, for example, exhibits the highest swelling among the membranes containing the alkali and alkaline earth metal ions (*13*, *14*).

Hydration energy of the counterion and the swelling of the membrane in water indicate how strongly a counterion is attached to the sulfonate group. Yeager and Steck (*13*) used powdered perfluorosulfonated ion-exchange resins to separate alkali metal ions and alkaline earth ions by column chromatography. They found the following order of univalent cation elution: Li Na K Rb Cs. Thus Cs^+ attaches to the resin material more strongly than Na^+ or H^+ attaches. One motivation of our using Cs^+ in this study was to find out if converting the membrane to the Cs^+ form caused a flux behavior different from the saturation kinetics.

The motivation for using Ag^+ was to see if we could obtain facilitation due to complexation with amino acids. In the absence of facilitation, one would expect lower fluxes than those obtained with the Na^+ membrane. This is because the hydration energy and swelling are lower for the Ag^+ membrane.

EXPERIMENTAL

1. Apparatus

Two permeation apparatus were used in this work. The first apparatus, a schematic of which is shown in Fig. 1, consisted of two 2-L glass boil-pots with short, 0.08 m diameter extensions attached to the pot-sides. The boil-pots were the two chambers of the permeation apparatus. The membrane was mounted vertically between the two chambers with a nylon coupling. The transport area was 3.85×10^{-3} m^2. Two agitators at 700 rpm stirred the solutions to minimize bulk diffusion effects. Temperature was maintained at 26°C by a heating mantle. Samples were collected from each cell at regular intervals after starting an experiment.

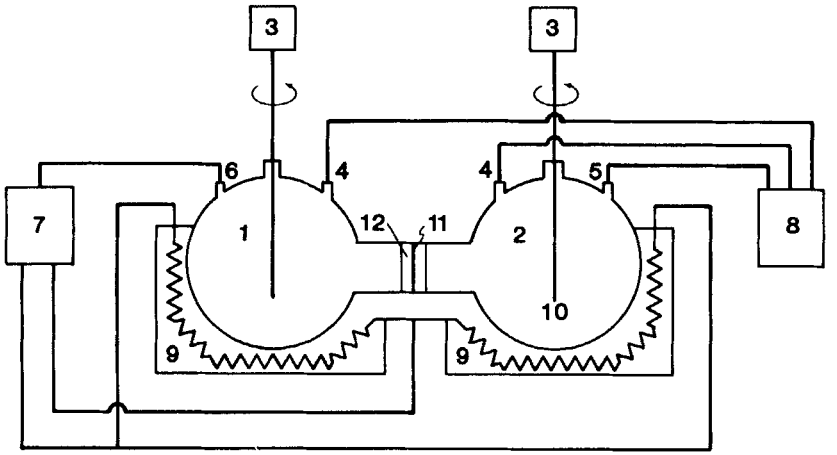

FIG. 1. Schematic of the old permeation apparatus. 1: Source chamber. 2: Sink chamber. 3: Agitater motor. 4: pH meter probe. 5: Temperature probe. 6: Temperature probe. 7: Temperature controller. 8: pH meter and display. 9: Electric mantle. 10: Stirrer. 11: Membrane. 12: Nylon connector.

Concentration was measured by a diode-array UV spectrophotometer. The first apparatus was operated near room temperature and at atmospheric pressure.

The second apparatus, similar in design to the first apparatus, contained two 750-mL, jacketed, stainless steel diffusion chambers. The apparatus was designed for operation at temperatures up to 70°C and pressures up to 270 kPa (25 psig). The membrane was mounted vertically on a narrow channel between two acrylic plastic pieces connected to the two chambers. Standard laboratory methods were applied for temperature control and pH measurement. Source and sink solutions were agitated by circulation pumps installed inside a control box. The pumping rate was such that a drop of a dye injected into the chambers reached equilibrium concentration in about 5 s. Samples were collected from the recycle lines. The transport area of the membrane was 20.27 cm^2. A schematic drawing of the second apparatus is shown in Fig. 2.

2. Membrane Treatment

The membrane, as received, was in the acid form. To assure a standard source material, we prepared the acid form of the experimental mem-

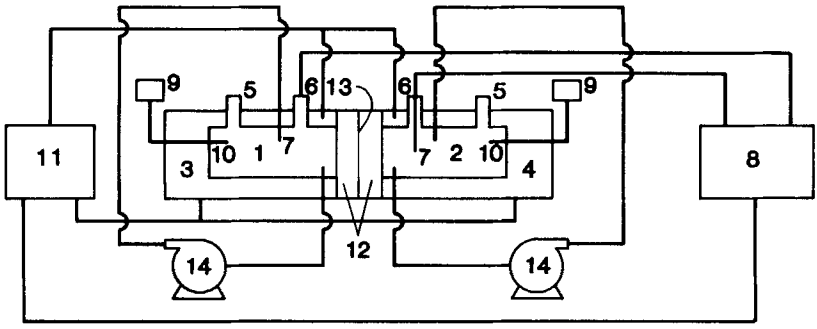

FIG. 2. Schematic of the new permation apparatus. 1: Source cell. 2: Sink cell. 3: Source jacket. 4: Sink jacket. 5: Orifice for sample. 6: Orifice for pH meter probe. 7: pH probe. 8: pH motor and pH display. 9: Temperature display. 10: Temperature probe. 11: Temperature controller. 12: Acrylic plastic connector. 13: Ion-exchange membrane. 14: Pump.

brane in the same manner described by Sikdar (*2*). The procedure included placing the membrane in a 0.5 mol/L H_2SO_4 solution and boiling for 2 h. This was followed by rinses with deionized water until the rinse water became neutral to pH.

The metal-substituted membranes were prepared by boiling an H^+ form in a solution containing the metal ion. The H^+ membrane had a rated equivalent mass% of 1100 and dry thickness of about 1.9×10^{-4} m. The concentrations of the electrolytes used to make the Na^+, Ag^+, and Cs^+ membranes were 1.25, 0.5, and 0.5 mol/L, respectively. The solutions containing the membrane were boiled for 2 h. Then each membrane was rinsed with deionized water until the rinse water showed neutral pH. Equivalent mass% of the metal-substituted membranes were determined from dry weights of both the H^+ and the metal-substituted forms of the membranes. The equivalent mass% provided a measure of the extent of substitution.

3. Experiments

The room temperature experiments were conducted in the first apparatus. Two liters of an aqueous solution of glycine were placed in the source chamber, while 2-L deionized water were placed in the sink chamber. The temperature was controlled at 26 ± 2°C. Each cell was agitated at 700 rpm with a laboratory stirrer.

Better temperature control (±0.1°C) was obtained in the second

apparatus. Experiments above room temperature were run in that apparatus. About 0.75-L aqueous solution of glycine was placed in the source chamber, and 0.75-L deionized water was placed in the sink chamber. Samples were collected after periodic intervals and were analyzed by a diode-array UV spectrophotometer at 208 nm wavelength.

Experiments were run at pH 6, the isoelectric pH for glycine. Experiments at pH's higher than the isoelectric pH were run only for the Na^+ membrane. In that case, sodium hydroxide solution was added to obtain alkaline pH's.

RESULTS AND DISCUSSION

Glycine concentration in the sink solution as a function of time is the typical raw data from an experiment. Such a data set for the Na^+ membrane at 26°C, pH 6, and for three different initial concentrations is presented in Fig. 3. These concentration vs time data were fitted with a second degree polynomial and differentiated at zero time to yield initial flux, J_i. In the following we will discuss, first, the effect of concentration on the initial fluxes of glycine for the Na^+ membrane; second, the effect of pH on glycine permeation through the Na^+ membrane; third, the

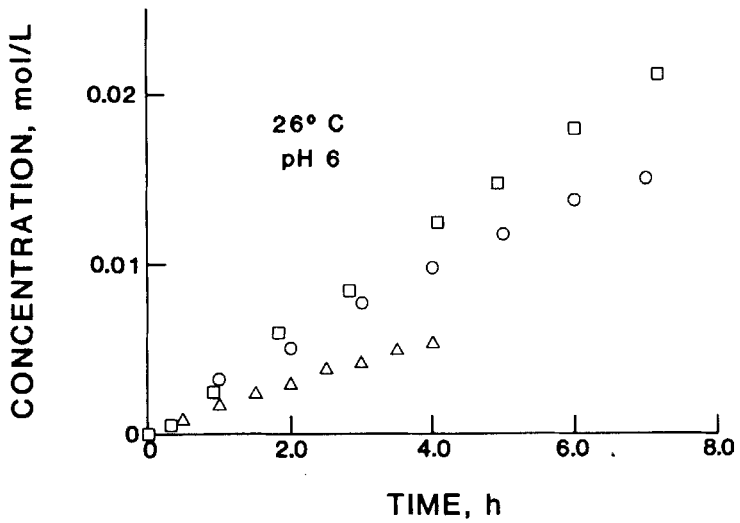

FIG. 3. Typical sink side concentration rise for glycine through the Na^+ membrane. Initial source concentrations are (△) 0.5 mol/L, (○) 1.5 mol/L, and (□) 2.0 mol/L.

activation energy of glycine transport; and, finally, the effect of counterions on the flux vs concentration relationship. For all the experiments discussed here, the sink side concentration at the beginning of an experiment was zero.

Like the previously reported alanine transport through the acid membrane (*3*), glycine exhibited saturation kinetics for both the H^+ and the Na^+ membrane. Figure 4 shows this result. The permeation through the acid membrane was significantly higher. Initial fluxes reached saturation for both membranes at a concentration slightly higher than 2 mol/L.

Saturation flux kinetics of the Michaelis-Menten type can be written in the form

$$J_i = \frac{J_m C}{K_m + C}$$

where J_i is the initial flux, mol/(cm^2 · s); J_m is the maximum attainable flux, mol/(cm^2 · s); K_m is the Michaelis-Menten constant; and C is the

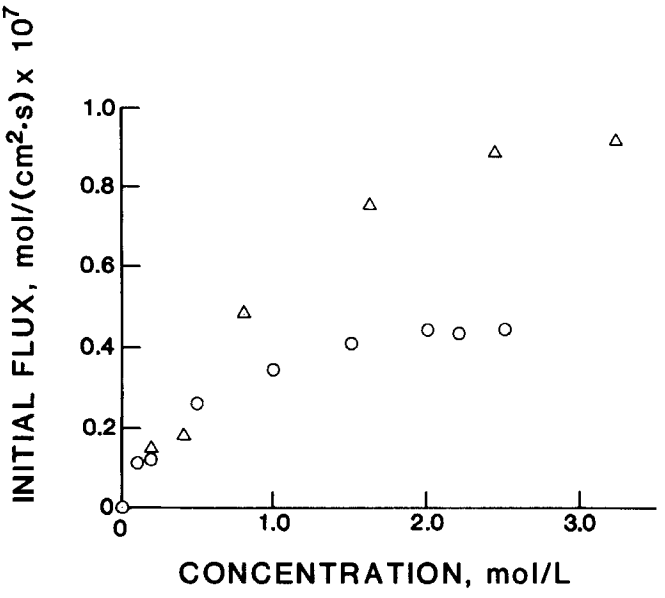

FIG. 4. Saturation flux kinetics of glycine for (△) H^+ membrane and (○) Na^+ membrane at 26°C.

molar concentration. K_m is the concentration which yields a flux equal to $J_m/2$. According to this equation, the transport flux is first order in concentration at low concentrations, and zero order at high concentrations.

Verification of these kinetics can be done by plotting $1/J_i$ vs $1/C$. The procedure yields a straight line, enabling one to determine the constants from the slope (K_m/J_m) and the intercept ($1/J_m$). Such a plot for the glycine transport through th Na^+ membrane is presented in Fig. 5. J_m and K_m for the Na^+ membrane at 26°C were 4.7×10^{-8} mol/(cm^2 · s) and 0.32 mol/L, respectively. The experimental data showing this effect of concentration on initial flux for glycine are presented in the first column of Table 1. The corresponding J_m and K_m data for the H^+ membrane were 1.3×10^{-7} mol/(cm^2 · s) and 1.7 mol/L, respectively. The data for the H^+ membrane, however, refer to a pH of 4.5 and a temperature of 25°C.

We now discuss the effect of pH on the glycine flux. Previous studies (*4*) showed that amino acid fluxes through the acid membranes were higher at pH's below the isoelectric pH than at pH's above the isoelectric pH. Glycine data of this work extend the previous study to alkaline pH's for the Na^+ membrane. The flux data of Table 2 show that the glycine flux at pH 12 was about half of that at pH 6. The concentration vs time data for

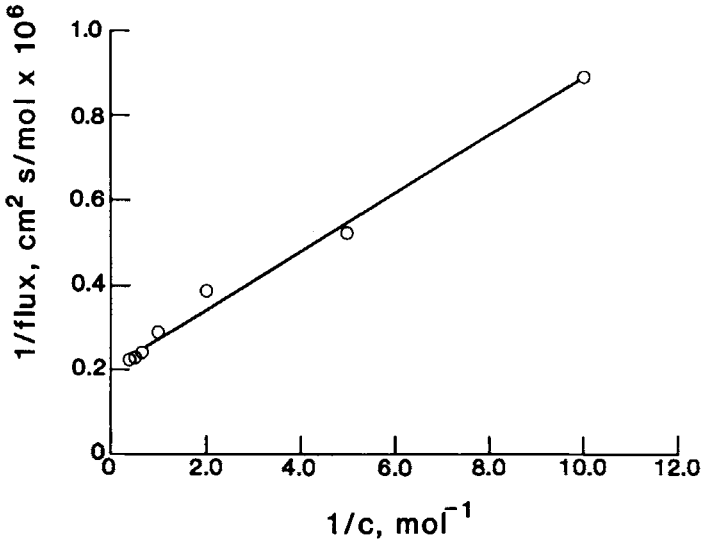

FIG. 5. Michaelis-Menten kinetics for glycine transport through Na^+ form of ion-exchange membrane at pH 6, 26°C.

TABLE 1
Glycine Fluxes Versus Source Concentration for Na^+, Ag^+, and Cs^+ Forms of Nafion 117 Membrane

	Fluxes [mol/(cm^2 · s) × 10^{-8}]		
Source concentration (mol/L)	Na^+ form	Ag^+ form	Cs^+ form
0.00	0.00	0.00	0.00
0.10	1.12	1.54	0.43
0.20	1.91	3.60	0.58
0.50	2.59	4.06	0.73
1.00	3.45	5.46	1.00
1.50	4.17	6.55	1.36
2.00	4.48	8.09	1.58
2.22	4.43		
2.50	4.48	9.16	1.74
3.00		9.91	1.98

the experiment at pH 12 are presented in Fig. 6. Similar data for NaOH alone at pH 13 and for glycine alone at pH 6 are also presented in Fig. 6 for comparison. We could not directly measure glycine flux at pH 12 since both glycine and sodium hydroxide absorbed at 208 nm UV wavelength. We needed to subtract the sodium hydroxide flux from the measured total flux of glycine and sodium hydroxide. Sodium hydroxide flux was computed from the sink side concentration measurement using atomic absorbance. The corrected glycine flux is in Table 2. We could not estimate the uncertainty in this measurement since we did not accurately know the NaOH source concentration in the experiment involving both glycine and NaOH. Only pH was measured, but pH is not a good measure of concentration at high alkalinity. Nonetheless, the reduction in the glycine flux at alkaline pH's was marked.

At pH 12, glycine is almost all in the anionic form. Since the membrane is cation exchange, ion exchange cannot be the mechanism of transport. We noticed that the sink pH increased very quickly during the experiment, indicating permeation of sodium hydroxide. We postulate that glycine moved through the membrane as the anion, with sodium ions copermeating to preserve the electrical neutrality of glycine.

We now discuss the effect of temperature on the glycine permeation through the Na^+ membrane. Figure 7 shows glycine transport data at three temperatures: 26, 35, 55°C. The initial source concentration for these runs were 2.0 mol/L and the source pH was 6.

The Arrhenius plot using the three initial flux data is shown in Fig. 8.

TABLE 2
Glycine, NaOH Transport through Na^+ Form of Nafion 117 Membrane Fluxes Data

Source	Glycine + NaOH		NaOH	Glycine
Concentration of glycine or NaOH	2.0 mol/L		2.0 mol/L	2.0 mol/L
pH of source	12		13	6
pH of sink	6		6	6
Temperature	26°C		26°C	26°C
Transported species	Glycine + NaOH		NaOH	Glycine
Flux	1.14×10^{-7} mol/(cm^2 · s)		1.0×10^{-7} mol/(cm^2 · s)	4.5×10^{-8} mol/(cm^2 · s)
	NaOH	Glycine		
	8.8×10^{-8} mol/(cm^2 · s)	2.6×10^{-8} mol/(cm^2 · s)		

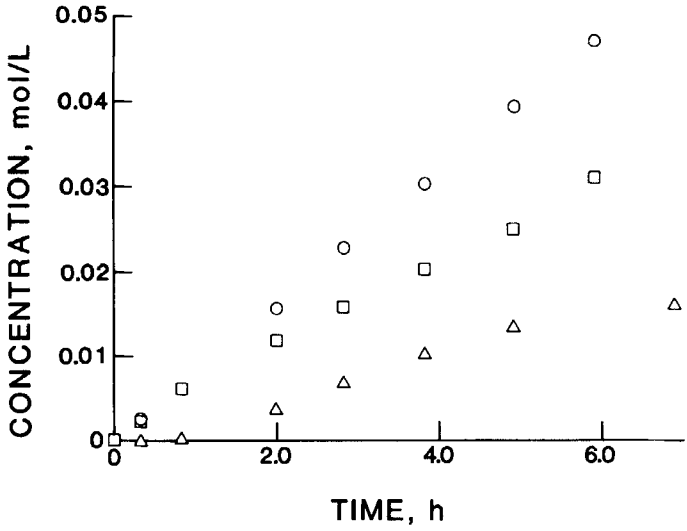

FIG. 6. Transient concentration on the sink side for (○) glycine + NaOH, (□) NaOH, (△) glycine.

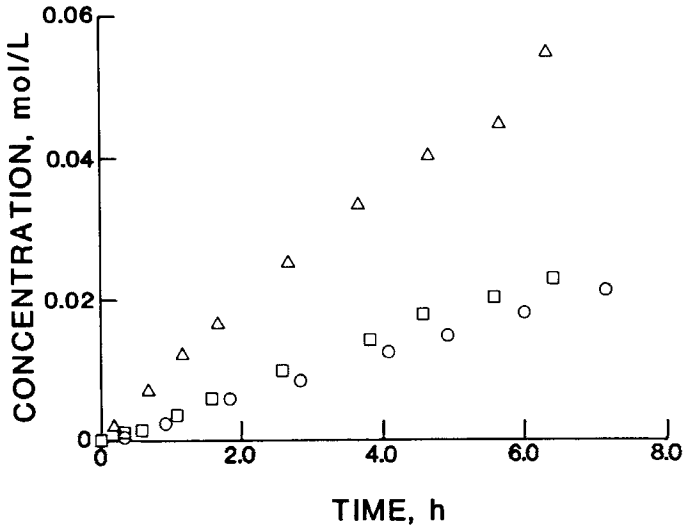

FIG. 7. Glycine permeation through the Na^+ membrane at (△) 55°C, (□) 35°C, and (○) 26°C. Initial source concentration 2.0 mol/L, pH 6.

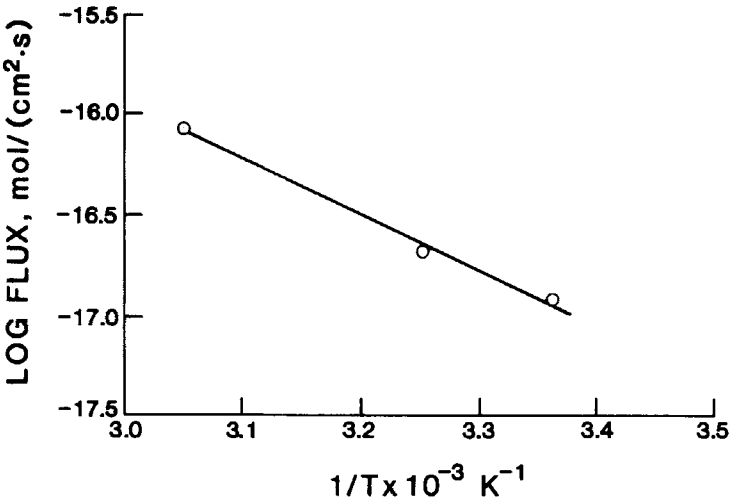

FIG. 8. Arrhenius plot of glycine transport through Na^+ membrane. Initial source concentration 2.0 mol/L, pH 6.

The activation energy of glycine transport for the Na^+ membrane, obtained from Fig. 8, was 23 kJ/mol (5.5 kcal/mol). The activation energy of glycine transport for the H^+ membrane was lower, 11.7 kJ/mol (2.8 kcal/mol). Both values are typical of diffisional processes. We have shown elsewhere (*5*) that at concentrations which caused flux saturation in the membrane, the activation energies are lower than those measured at lower concentrations. The higher activation energies at lower concentrations indicate chemical interaction of the transport species with the ion-exchange membrane.

Last, we discuss the effect of counterions on the flux behavior of glycine. We explained earlier that the counterion determined hydration number and membrane swelling. We wanted to find out whether the fluxes correlated with the hydration number and hence with the counterion In Fig. 9 we show how the initial fluxes of glycine for the Ag^+, Na^+, and Cs^+ membranes varied with concentration.

The fluxes through the Na^+ membrane represent the Michaelis-Menten type saturation kinetics, as discussed before. The flux data for the Cs^+ membrane were qualitatively different from those of the Na^+ membrane. For the Cs^+ membrane, the fluxes were much lower and the concentration dependence was approximately Fickian; that is, the flux increased linearly with concentration. The Ag^+ membrane behaved

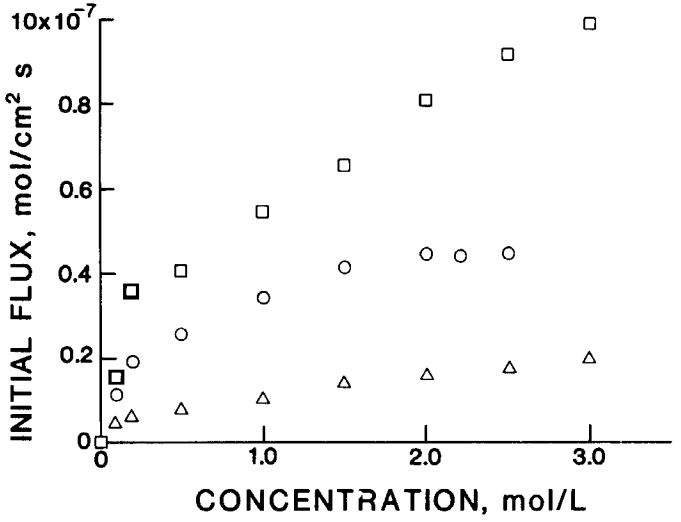

FIG. 9. Effect of counterions on flux-concentration behavior: (□) Ag^+ membrane, (○) Na^+ membrane, (△) Cs^+ membrane. 26°C, pH 6.

differently still. The flux increased rapidly with concentration at first, and then followed a Fickian trend at higher concentrations. We could not detect any tendency for the fluxes to saturate even at an initial concentration of 3.0 mol/L, whereas the Na^+ membrane saturated at a concentration slightly higher than 2.0 mol/L.

In Table 3 we present a capsule comparison of the glycine flux behaviors for the H^+, Na^+, Cs^+, and Ag^+ membranes. The hydration numbers given in the last column appeared to correlate generally with the fluxes. Higher hydration number indicate greater swelling of the ion clusters and a higher degree of ion-exchange ability. The more mobile the counterions, the greater were the glycine fluxes. The hydration numbers used here were reported for ion-exchange resins (*12*). We tacitly assumed that the parallelism held for ion-exchange membranes.

The Cs^+ membrane exhibited the least ionization (as evident from the hydration number of 0) and the least water swelling of the four membranes we studied. The nearly Fickian behavior suggests that the membrane was not a good ion exchanger.

The Ag^+ membrane exhibited higher flux than the Na^+ membrane although its hydration number (0.3) was much lower. The most likely explanation is that Ag^+ complexes with glycine, thus compensating for its lower hydration number.

TABLE 3
Glycine Flux Behaviors of Membranes

Nafion membrane form	Initial flux $\times 10^8$ mol/(s · cm^2)	Equivalent weight	Swollen thickness (m)	Hydration number[a]
H^+	13	1100	223	3.9
Na^+	4.5	964	214	1.5
Ag^+	8.0	1174	206	0.3
Cs^+	1.6	1054	203	0

[a]From Ref. *12*.

The Ag^+ membrane also exhibited a composite flux behavior: at low concentration the flux vs concentration data were nonlinear, and at higher concentration the data were linear. This phenomenon can be explained in the following way.

We need to consider two kinds of fluxes: one due to Fickian diffusion and the other due to interaction with the membrane. For any of the membranes we used, both components were present; one may have overshadowed the other, or sometimes both may have been dominant. We postulate that the glycine fluxes, for the acid and sodium membranes which are good ion exchangers, resulted primarily from a reversible interaction of glycine with the membranes, resulting in higher glycine solubility in the membrane. Since chemical interaction was faster in these two membranes, as would be expected for equilibrium control, the Fickian driving force across the membrane was very small. The cesium membrane, in contrast, did not appreciably interact with glycine. As a result, the flux was predominantly Fickian.

However, the fluxes for the silver membrane were somewhere between the two extremes. At low concentrations, both diffusion and chemical interaction fluxes were comparable. The competition between these two fluxes caused the curvature at low concentrations in Fig. 9. At higher concentrations still, the diffusive flux became dominant, and the combined flux kept on increasing with increasing concentration.

CONCLUSION

The most significant result of this study came from a comparison of the glycine flux behaviors in the membranes having metallic counterions. The H^+ and Na^+ membranes both exhibited saturation kinetics of the transport flux, indicating interaction of glycine with the membrane sulfonate sites. The Ag^+ and Cs^+ membranes, with significantly smaller counterion hydration numbers, offered different transport behavior. In neither case could we detect flux saturation.

The absence of flux saturation for Ag^+ and Cs^+ membranes appears to result from reduced interaction between glycine and the membrane. We postulate that this reduced interaction is a direct result of low ionizability of the sulfonates in these membranes. We saw that higher ionizability of the sulfonates, for example, Na^+, led to higher glycine flux and resulted in Michaelis-Menten type saturation flux kinetics.

REFERENCES

1. H. L. Chum, A. K. Hauser and D. Sopher, "New Uses of Nafion Membranes in Electroorganic Synthesis and in Organic Acid Separation," *J. Electrochem. Soc.*, p. 2508 (December 1985).
2. S. K. Sikdar, "Transport of Organic Acids through Perfluorosulfonated Polymeric Membranes," *J. Membr. Sci., 23*(1), 83 (1985).
3. S. K. Sikdar, "Amino Acid Transport from Aqueous Solutions by a Perfluorosulfonic Acid Membrane," *Ibid., 24*(1), 59 (1985).
4. S. K. Sikdar, "Permeation Characteristics of Amino Acids through Perfluorosulfonated Polymeric Membranes," *Ind. Eng. Chem. Res., 26*(1), 170 (1987).
5. S. K. Sikdar, "Saturation Kinetics of Acetic Acid Transport through Perfluorosulfonated Ion-Exchange Membranes," *Sep. Sci. Technol., 21*(9), 941 (1986).
6. A. Steck and H. L. Yeager, "Water Sorption and Cation-Exchange Selectivity of a Perfluorosulfonate Ion-Exchange Polymer," *Anal. Chem., 52,* 1215 (1980).
7. S. Grot, G. Munn, and P. Walmsley, *Perfluorinated Ion-Exchange Membranes,* Presented at the 141st National Meeting of the Electrochemical Society, Houston, Texas, May 7-11, 1972.
8. A. Narebska and R. Wodzki, *Angew. Makromol. Chem., 107,* 51 (1982).
9. T. Gierke and Y. Hsu, "The Cluster-Network Model of Ion Clustering in Perfluorosulfonated Membranes," in *Perfluorinated Ionomer Membranes* (ACS Symp. Series 180), American Chemical Society, Washington, D.C., 1982, p. 283.
10. H. Yeager and A. Steck, "Cation and Water Diffusion in Nafion Ion Exchange Membranes: Influence of Polymer Structure," *J. Electrochem. Soc., 128,* 1880 (1981).
11. W. Hsu, J. Barkley, and P. Meakin, "Ion Percolation and Insulator-to-Conductor Transition in Nafion perfluorosulfonic Acid Membranes," *Macromolecules, 13,* 198 (1980).
12. F. Hellerich, *Ion Exchange,* McGraw-Hill, New York, 1962.
13. H. Yeager and A. Steck, "Ion Exchange Selectivity and Metal Ion Separations with a Perfluorinated Cation Exchange Polymer," *Anal. Chem., 51,* 862 (1979).
14. G. Eisenman, "Cation Selective Glass Electrodes and Their Mode of Operation," *Biophys. J., 2,* 259 (1962).

Received by editor November 18, 1987